Atmospheric Environment 45 (2011) 6546–6556

Contents lists available at SciVerse ScienceDirect

Atmospheric Environment

journal homepage: www.elsevier.com/locate/atmosenv

Predicted changes in summertime organic aerosol concentrations due to increased temperatures

Melissa C. Day [a], Spyros N. Pandis [a,b,*]

[a] Department of Chemical Engineering, Carnegie Mellon University, 5000 Forbes Ave., Pittsburgh, PA 15213, USA
[b] Department of Chemical Engineering, University of Patras, Patra, Greece

ARTICLE INFO

Article history:
Received 14 May 2011
Received in revised form
9 August 2011
Accepted 10 August 2011

Keywords:
Climate change
Air quality
Organic aerosol
Volatility basis set
Modeling
PMCAMx

ABSTRACT

Changes in summertime organic aerosol (OA) concentrations in the Eastern U.S. are investigated for different temperature change scenarios using the chemical transport model PMCAMx-2008. OA is simulated using the volatility basis set approach, assuming that the primary emissions are semi-volatile and that the intermediate volatile and semi-volatile organic compounds are oxidized in the gas phase, resulting in products with lower volatility. For the basic temperature change scenario where biogenic emissions are kept constant, ground-level OA decreases by $-0.3\%\ K^{-1}$ on average. Increases in the north ($+0.1\%\ K^{-1}$) and decreases in the south ($-0.5\%\ K^{-1}$) are predicted. The effect of the uncertain temperature dependence of the aging rate constant is modest, changing the OA by only $0.1\%\ K^{-1}$ over the temperature-independent case. For the more realistic scenario in which biogenic OA precursor emissions are allowed to increase with temperature (up to $10\%\ K^{-1}$), however, average OA increases by $4.1\%\ K^{-1}$, with even higher increases in southern regions. These results suggest that as temperature increases, complicated changes in production, partitioning and chemical aging will take place. Nevertheless, the change in biogenic emissions and subsequent production of biogenic OA is more than an order of magnitude more important than the changes in the rates of chemical and physical atmospheric processes.

1. Introduction

Elevated particulate matter (PM) concentrations contribute to poor air quality throughout large parts of the United States. These particles directly affect visibility and have been linked to increased risks of respiratory illness and cardiopulmonary disease (Dockery et al., 1994; Davidson et al., 2005). $PM_{2.5}$, particles with an aerodynamic diameter less than 2.5 μm, are particularly important as they can travel far into the human respiratory system and are therefore more dangerous than larger particles.

Airborne particles, or aerosols, are traditionally grouped in two categories based on their origin. Primary aerosols refer to those emitted directly into the atmosphere, such as sea salt and dust; secondary aerosols begin as gas-phase compounds emitted by transportation, industry, vegetation and other sources. These gases are then oxidized in the atmosphere, resulting in products that can condense to the particle phase, forming secondary aerosol. Organic aerosol constitutes a significant portion of $PM_{2.5}$ mass in both urban and rural areas (Seinfeld and Pandis, 2006), and has been traditionally categorized as primary (POA) and secondary organic aerosol (SOA). The behavior of anthropogenic (aSOA) and biogenic (bSOA) secondary organic aerosol – from manmade and natural sources, respectively – has been the subject of investigation in both laboratory and modeling studies (Kanakidou et al., 2005).

A 1.5–4.5 K rise in the global average surface temperature is predicted for the next century (IPCC, 2007). While a number of studies have concluded that increased temperatures result in higher ozone concentrations for both present and future simulations (Aw and Kleeman, 2003; Baertsch-Ritter et al., 2004; Jacob and Winner, 2009), $PM_{2.5}$ behavior predicted by different global models for future temperature or climate scenarios is inconsistent (Jacob and Winner, 2009). There are also few publications describing the effect of climate on organic PM levels regionally. Using direct secondary organic aerosol modeling of winter conditions in central California, Strader et al. (1999) predicted there would be an optimal temperature for SOA formation due to the interplay between particle evaporation and accelerated chemistry as temperature increases. An increase of 10 K from this optimum

* Corresponding author. Department of Chemical Engineering, Carnegie Mellon University, 5000 Forbes Ave., Pittsburgh, PA 15213, USA. Tel.: +1 412 268 3531; fax: +1 412 268 7139.
E-mail address: spyros@andrew.cmu.edu (S.N. Pandis).

1352-2310/$ – see front matter © 2011 Elsevier Ltd. All rights reserved.
doi:10.1016/j.atmosenv.2011.08.028

decreased SOA by 18% (1.8% K^{-1}). A similar effect was predicted by Aw and Kleeman (2003) via a Lagrangian trajectory model for secondary organic compounds in Southern California for September 1996. Secondary organic particulate matter decreased by about 1% K^{-1} for their temperature perturbation trials. The chemical transport model PMCAMx predicted that the organic $PM_{2.5}$ for the eastern U.S. in July 2001 would decrease by about 0.75% K^{-1} (Dawson et al., 2007). Sheehan and Bowman (2001) predicted a 16 and 24% decrease in SOA during the day with a temperature increase of 10 K (−1.6 and −2.4% K^{-1}) from the reaction of high-yield aromatics and alpha-pinene, respectively, with OH. SOA formation was simulated with a single cell absorptive partitioning box model. Although the magnitude of the temperature effect is relatively consistent between these earlier studies, constant biogenic emissions and nonvolatile non-reactive POA were assumed for these simulations.

Tai et al. (2010) analyzed an 11-year (1998–2008) record of $PM_{2.5}$ observations finding a positive concentration correlation (approximately 0–7% K^{-1}) in organic carbon (OC) with temperature in the eastern U.S., except in southern Florida where a negative relationship was observed. Meteorological variables explained up to 50% of the observed daily $PM_{2.5}$ variability; the study suggested that the temperature dependence of biogenic emissions and wildfires were also important factors for the OC increase with temperature. VOC emissions from vegetation in the US are comparable to those from anthropogenic sources (Guenther et al., 1993; Lamb et al., 1987). Leaitch et al. (in press) reported that submicron forest OA in Canadian forests correlated to ambient temperature via the equation $OA = 0.084\exp(0.135\ T)$, with temperature in °C and concentration in μg m^{-3}. This corresponds to 13.5% K^{-1}. Guenther et al. (1993) reported an exponential increase in monoterpene emissions with temperature. In the same study, isoprene emissions were found to increase for leaf temperatures up to 40 °C decreasing thereafter. Between 25 and 35 °C, an increase on order of 10% K^{-1} can be estimated for both monoterpenes and isoprene. For the same temperature range, other studies implied that isoprene emissions could increase by about 6% K^{-1} (Duncan et al., 2009), and yet others reported a 27% K^{-1} increase (Sharkey et al., 2008). Constable et al. (1999) estimated a 13% K^{-1} increase for biogenic emissions, including isoprene, monoterpenes, and other reactive VOCs. Although the exact response is uncertain, it is evident that biogenic emissions do change significantly with temperature.

Recent developments in our understanding of atmospheric OA physics and chemistry (Robinson et al., 2007) have shown that other elements of OA treatment by previous chemical transport models (CTMs) require further revision. POA was historically viewed as nonvolatile and non-reactive, but it is now clear that a significant fraction evaporates after emission. The resulting vapors participate in atmospheric reactions that ultimately lead to the formation of oxidized OA. Furthermore, both volatile POA and SOA components and precursors are influenced by chemical aging, or further gas phase oxidation of the first-generation products of OA chemistry (Donahue et al., 2006). The inclusion of intermediate volatility organic compounds (IVOCs; Grieshop et al., 2009) and updated SOA formation yields (Hildebrandt et al., 2009; Murphy and Pandis, 2010) have also led to improved prediction accuracy (Murphy and Pandis, 2009). The previous work on the climate sensitivity of OA has neglected these effects.

PMCAMx, a regional scale CTM, used the Odum et al. (1996) two-product framework to simulate organic aerosol concentrations as described by Gaydos et al. (2007). Dawson et al. (2009), which is the precursor to this work, used this model to calculate OA sensitivity to temperature and biogenic emissions. This model has been subsequently modified to include the volatility basis set (Lane et al., 2008; Shrivastava et al., 2008). This version is a significant advancement in OA prediction methodology within PMCAMx, and it is now necessary to revisit past applications and see how the estimates about the role of temperature have changed.

We will quantify the temperature effect using three scenario groups; one in which only select processes are temperature dependent, one that adds temperature sensitivity to the semi-volatile organic gas aging rate constant and one where biogenic emissions increase with temperature. These three groups seek to add realism to the model beyond the gas-aerosol partitioning, species reaction rates and deposition rates that are already temperature-sensitive. The first group has been simulated before, but never with the volatility basis set framework. The temperature sensitivity of chemical aging, the second group, is quite uncertain and bears examination. Finally, from the wide variation of biogenic emission temperature sensitivity in the literature, reasonable values are used to explore this effect in the new model.

2. Model description

The thousands of mostly unknown species in ambient OA are represented by surrogate organic compounds with a range of volatilities in PMCAMx-2008. In the volatility basis set framework, the volatility of these surrogate organic compounds is represented by C^*, the effective saturation concentration at 298 K, and logarithmically spaced bins are used to simulate the OA volatility distributions (Donahue et al., 2006). At 298 K, these bins span the range from 10^{-2}–10^{6} μg m^{-3} for POA and 1–10^{4} μg m^{-3} for SOA, enabling the model to simulate the wide range of volatility in atmospheric organics. C^* is temperature-dependent as described by the Clausius–Clapeyron equation. Species parameters, including molecular weights and enthalpies of vaporization, are provided in Murphy and Pandis (2009) supporting information; ΔH_{vap} is 30 kJ mol^{-1} for SOA and between 64 and 112 kJ mol^{-1} for POA. The enthalpies, especially for SOA, are uncertain (Epstein et al., 2010), but are consistent with the few available smog chamber experiments that explored the temperature dependence of the SOA yields. The chemical aging mechanism simulates the reduction of the organic vapor volatility by an order of magnitude, or a shift to one C^* bin lower, creating products that are less volatile than the parent compound (Lane et al., 2008; Shrivastava et al., 2008). Murphy and Pandis (2009) formulated PMCAMx-2008, which includes the volatility basis set framework for both POA and SOA in addition to chemical aging of POA and anthropogenic SOA. Biogenic aging is assumed to lead to a negligible change of the corresponding yields. Lane et al. (2008) concluded that assuming bSOA components react in the gas phase with OH with a rate constant equal to 4×10^{-12} cm^{-3} $molecule^{-1}$ s^{-1} results in significant overprediction of the observed OA in rural areas (e.g., in the southeast US). Murphy and Pandis (2009) showed that PMCAMx, assuming that the effect of the chemical aging of the bSOA on its concentration is negligible, was able to reproduce well the summertime OA concentration field in the Eastern US. Murphy and Pandis (2010) explored a series of aging scenarios, showing that the current aging scheme (increasing aSOA yields and constant bSOA yields with aging) resulted in the best performance. Based on these results we have kept the base case parameters of Murphy and Pandis (2009) for the present study.

PMCAMx-2008 simulations were performed for a 3492 × 3240 km area over the eastern half of the United States. This domain was gridded into 36 × 36 km cells, resulting in a subdivision of 97 cells (east-west) by 90 cells (north-south). Also included are 14 vertical layers extending to 6 km above the surface. The boundary OA concentration is set to 0.8 μg m^{-3} for the first 10 model layers (~2 km) and 0.3 μg m^{-3} for layers 11–14 (~2–6 km) following Karydis et al. (2007). The SAPRC-99 (Statewide Air Pollution Research

Center) photochemical mechanism (Carter, 2000) was used for molecularly lumped gas-phase chemistry calculations with all reactions having temperature-dependent reaction rate constants. This replaced the Carbon-Bond Mechanism (CBM) IV (Gery et al., 1989) that was used in the original studies by Dawson et al. (2007, 2008, 2009) with PMCAMx-2002. Inorganic aerosol thermodynamics are described by ISORROPIA (Nenes et al., 1998) and are affected by temperature. Equilibrium partitioning between the gas and particle phases – also temperature-dependent – is assumed for both inorganic and organic aerosol components. Rain intensity, photochemical intensity, height and pressure were input via the fifth-generation mesoscale model (MM5; Grell et al., 1995 as described in Gaydos et al., 2007) to PMCAMx. Anthropogenic point and area emissions are based on the U.S. National Emissions Inventory (NEI) databases, and biogenic emissions are from the Biogenic Emissions Inventory System version 3.13 (Schwede et al., 2005). Further details of the modeling framework are described in Gaydos et al. (2007).

For each modeling scenario, seventeen days between 12 and 28 July 2001 were simulated. The first two days of each simulation are used for initialization and are not included in subsequent analysis of the results (Karydis et al., 2007). In addition to a base-case scenario, several scenarios were simulated in order to analyze different aspects of the temperature effect on OA levels (Table 1). Uniform temperature increases of +2.5 and +5 K were applied across the entire simulation, including all layers. These values represent medium and high climate change temperature increase estimates according to the IPCC. Such a consistent increase is clearly a simplification so this should only be viewed as a sensitivity test. For AGE simulations, the anthropogenic SOA (aSOA) and oxidized POA (oPOA) aging rates were made temperature-dependent by the addition of an E_a/R value of 500 K in the Arrhenius equation, where E_a is the activation energy and R is the ideal gas constant. Finally, biogenic precursor emissions in the BIO simulations were increased by 5% K^{-1} or 10% K^{-1} for the corresponding temperature increase scenarios.

3. Results and discussion

3.1. Baseline model performance

The base case average surface concentration predictions for total OA are shown in Fig. 1 along with the fractional contributions of its constituents. Here, gas-aerosol partitioning and gas phase reaction rate constants are temperature-sensitive but the aging rate constant is not. This model is only slightly modified (coding improvements) from Murphy and Pandis (2010). The fresh POA (fPOA) is present mostly near urban and industrial centers, with contributions up to 16%. Oxidized POA and anthropogenic SOA have high contributions over most of the domain with peaks of 20% and 60% in the Midwest, respectively. The biogenic SOA has its highest values, with a maximum 72% contribution, in the southern U.S. Finally, the OA from long range transport is 0.4 μg m^{-3} on average and covers the entire domain, contributing almost all of the OA near the boundaries where the concentration is low.

These OA predictions were compared to measurements from the Speciation Trends Network (STN) (US EPA, 2002) and the Interagency for Monitoring of Protected Visual Environments (IMPROVE) (IMPROVE, 1995) stations. The STN data include both urban and suburban sites, whereas most of the IMPROVE sites are in rural locations. Measurements of aerosol organic carbon (OC) were converted to OM for comparison; IMPROVE OC data were multiplied by 1.8 to reflect the more highly oxidized nature of emissions at rural sites, while STN OC data were multiplied by 1.4 as urban OA is generally less aged or oxidized (Simon et al., 2011; Zhang et al., 2005). A blank-correction was also applied to the STN data (Chow et al., 2001).

Whereas PMCAMx-2002 generally underpredicted organic matter (Karydis et al., 2007), especially in urban (STN) sites, PMCAMx-2008 exhibits improved behavior. When compared to measurements, PMCAMx-2002 predictions had a fractional error of 0.63 and a fractional bias of −0.57 for the urban (STN) sites; PMCAMx-2008 results show a fractional error of 0.42 and a fractional bias of only 0.09. PMCAMx-2008 tends to slightly overpredict OA for the rural (IMPROVE) sites resulting in a fractional bias equal to 0.3, but the fractional error decreased from 0.43 to 0.39. A more extensive comparison of PMCAMx-2008 predictions to measurements can be found in Murphy and Pandis (2010).

3.2. Effects of temperature on OA

The concentration differences between the 5 K increase simulation (TEMP + 5) and the base case for the total OA are shown in Fig. 2; corresponding percentage changes are shown in Table 2. Across the entire domain, total OA decreases by 1.5% on average at ground level. There are two distinct regions of change, however. The north and south boxes in Fig. 2 were chosen to isolate this behavior. On average, the south shows a decrease of 2.6% and the north exhibits a 0.7% increase. These concentration changes are supplemented by results from specific example cities in Table 2. The

Table 1
PMCAMx-2008 scenarios simulated in this work.

Scenario	Temperature perturbation	Dependence on temperature		
		Gas-phase chemistry; deposition; aerosol partitioning	Semivolatile aging rate constant	Biogenic emissions
Base	None. Base case temperature fields	Yes	No	Base case
TEMP + 2.5	+2.5 K uniform increase	Yes	No	Base case
TEMP + 5	+5 K uniform increase	Yes	No	Base case
AGE_base	None. Base case temperature fields	Yes	Yes, aSOA and oPOA aging rate with $E_a/R = 500$ K	Base case
AGE + 5	+5 K uniform increase	Yes	Yes, aSOA and oPOA aging rate with $E_a/R = 500$ K	Base case
BIO25 + 2.5	+2.5 K uniform increase	Yes	No	Yes, 25% biogenic precursor emissions increase
BIO25 + 5	+5 K uniform increase	Yes	No	Yes, 25% biogenic precursor emissions increase
BIO50 + 5	+5 K uniform increase	Yes	No	Yes. 50% biogenic precursor emissions increase

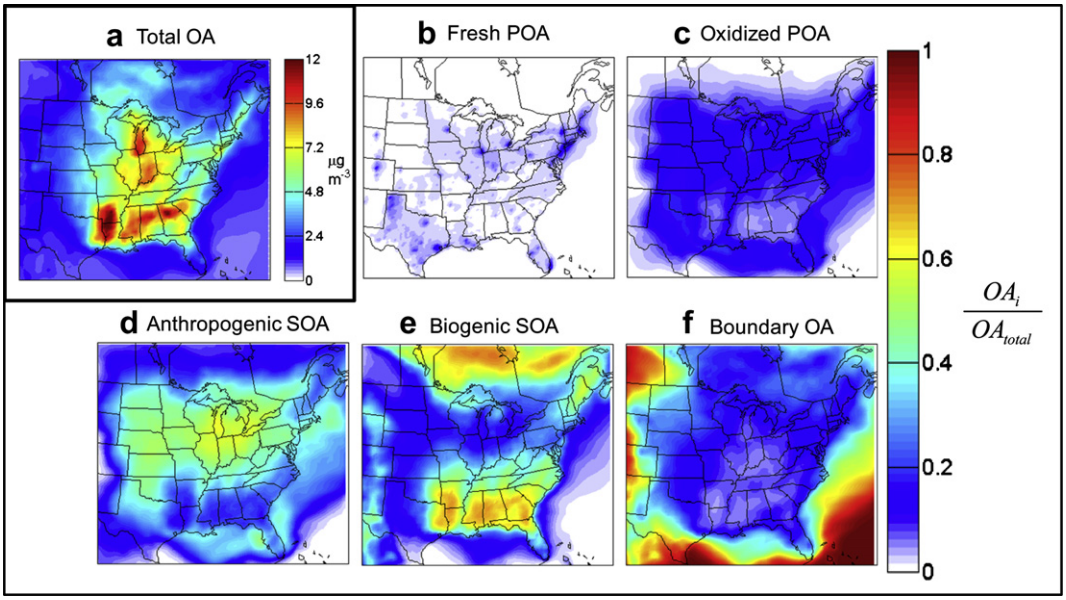

Fig. 1. (a) Base-case predicted average surface concentrations (μg m^{-3}) during July 2001 for total organic aerosol, and fractional contributions of the OA components – (b) fresh POA, (c) oxidized POA, (d) anthropogenic SOA, (e) biogenic SOA, and (f) boundary condition OA representing the organic aerosol transport into the domain from other areas.

three southern cities – Atlanta, GA, Hattiesburg, MS, Shreveport, LA – were chosen based on their proximity to areas with the largest concentration change. These sites show OA base concentrations well above the southern average, and the concentration decreases up to 4.2%, showing that the local temperature effect can be much stronger than average. Of the three northern cities chosen for inspection, Cincinnati, OH shows a higher than average concentration change (1.5%), but both Chicago, IL and Pittsburgh, PA show a slight decrease in concentration with temperature. The local effect in the north is therefore more varied.

The causes of these north-south differences can be explained by the behavior of the OA components, shown in Fig. 3. On average, bSOA decreases across the domain by 0.1 μg m^{-3}, a 4% drop from the base case bSOA. Maximum reductions up to 0.5 μg m^{-3} in the south are observed, and decreases are also predicted for the northeastern U.S. and Canada. The fresh POA (fPOA) is also predicted to decrease, with average reductions of 0.02 μg m^{-3} (13% decrease) and maximum reductions up to 0.2 μg m^{-3} at urban centers. In contrast, anthropogenic SOA responds to higher temperatures by increasing 0.1 μg m^{-3} or 5% on average, with a maximum of 0.2 μg m^{-3} in the Midwest. Oxidized POA exhibits the same effect with a small average increase of 0.03 μg m^{-3} (+5%) and a maximum of 0.12 μg m^{-3}.

These changes are due to a combination of factors related to increasing temperature. To identify these, it is useful to examine how the volatility distributions and partitioning of the OA components between the gas and particle phases changes with temperature. The differences in the OA volatility distributions between the +5 K runs and base case are shown in Fig. 4. The SOA parent hydrocarbon reactions accelerate with temperature, leading to increases in the total concentration in all bins for both aSOA and bSOA (Fig. 4a and b). Contrary to aSOA, which will be described shortly, most of the additional bSOA material stays in the gas phase along with additional bSOA that evaporates. As a result, the concentrations of the gas phase bSOA components increase and the particulate bSOA components decrease across all volatility bins (Fig. 4a). Although the scale of the changes is reduced, increases in gas (all bins) and decreases in aerosol (for $C^* \leq 10^3$ μg m^{-3}) are also seen with the fPOA (Fig. 4c). Evaporation of lower-volatility fPOA increases gas levels and decreases aerosol concentrations; subsequent loss to oPOA formation occurs as

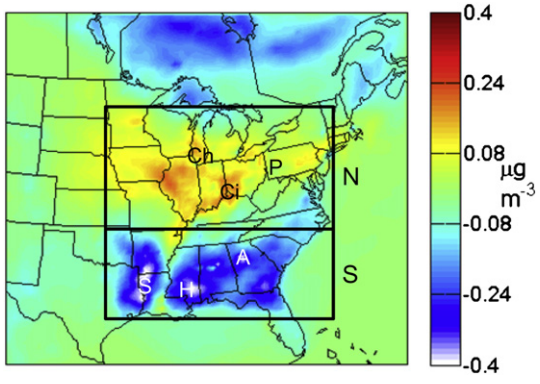

Fig. 2. Concentration differences (in μg m^{-3}) between TEMP + 5, the +5 K temperature simulation, and the Base case for total OM and associated cities; Shreveport (S), Hattiesburg (H), Atlanta (A), Chicago (Ch), Cincinnati (Ci) and Pittsburgh (P). Also shown are the north and south box boundaries, used to obtain a closer analysis of our results.

Table 2
Predicted total OA changes in select cities for the TEMP + 5 and BIO scenarios.

Site	Base concentration, μg m^{-3}	% Difference between specified run and base			
		TEMP + 5	BIO25 + 2.5	BIO25 + 5	BIO50 + 5
Average	3.1	−1.5%	9.9%	8.9%	20.5%
South average	5.8	−2.6%	17.3%	15.5%	36.1%
Hattiesburg, MS	9.1	−4.2%	22.0%	19.3%	45.6%
Atlanta, GA	11.8	−3.3%	18.8%	16.5%	38.6%
Shreveport, LA	11.1	−3.3%	22.5%	20.5%	47.1%
North average	6.5	0.7%	6.2%	6.6%	13.0%
Cincinnati, OH	8.1	1.5%	8.1%	9.0%	16.5%
Pittsburgh, PA	6.0	−0.3%	5.6%	5.5%	11.5%
Chicago, IL	10.5	−0.1%	3.1%	3.3%	6.5%

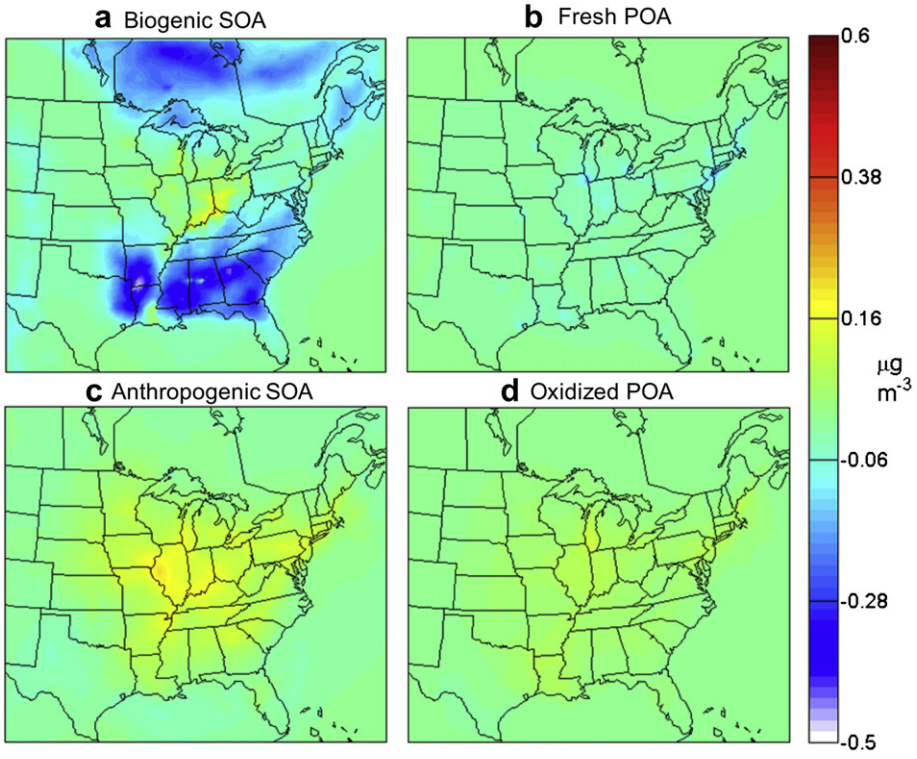

Fig. 3. Average surface organic aerosol concentration differences (in μg m^{-3}) between TEMP + 5, the +5 K simulation, and the Base case for (a) bSOA, (b) fPOA, (c) aSOA, and (d) oPOA. Positive changes correspond to increases in OA with increasing temperature.

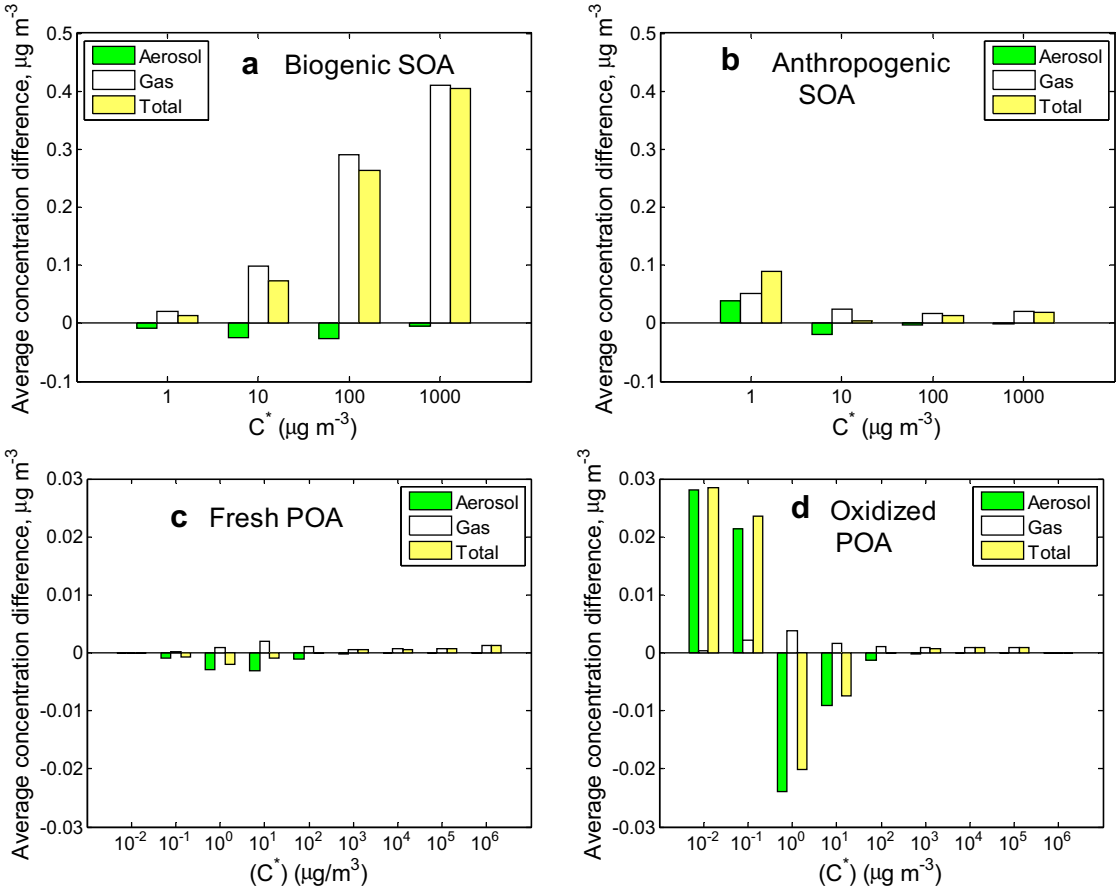

Fig. 4. Changes in volatility distributions due to increased temperature for (a) bSOA, (b) fPOA, (c) aSOA, and (d) oPOA. The difference between TEMP + 5, the +5 K simulation, and the Base case are shown. Different scales are used for SOA and POA.

temperature increases and gas-phase aging is enhanced. Gas-phase fPOA surrogate species also have temperature-dependent Henry's Law coefficients; an increase in temperature decreases their water solubility and therefore dry and wet deposition rates, leading to a small increase in the concentrations of the high-volatility fPOA components.

Aging reactions differentiate the changes in aSOA and oPOA volatility distributions from those of bSOA and fPOA (Fig. 4b and d). In addition to an increase in gas due to evaporation for both species, an increase in lower volatility aerosol can be seen. When OA partitioning is shifted into the gas phase, more material becomes available for gas-phase aging reactions with OH, creating products that are less volatile than the parent. This in turn produces higher aSOA and oPOA levels in the lower volatility bins. So far, the model assumes that the rate constants of the aging reactions are temperature independent, but it is clear that chemical aging of OA amplifies the effect of a temperature increase.

3.3. Temperature-dependent anthropogenic aging rate constant

Temperature-independent aging reaction rate constants have been used in previous OA chemical aging studies (Shrivastava et al., 2008; Murphy and Pandis, 2009) and in the studies discussed above. There is little available information on possible temperature sensitivity of these processes, however. To test the system we use an activation energy E_a/R of 500 K, which is higher than all related anthropogenic species activation energies in SAPRC99, for the aging process across all bins. This approximately corresponds to a 0.6% K^{-1} change in the reaction rate. The reference temperature is 298 K, at which point the rate constant equals 1×10^{-11} cm^3 $molecule^{-1}$ s^{-1} for aSOA and 4×10^{-11} cm^3 $molecule^{-1}$ s^{-1} for oPOA as determined by Murphy and Pandis (2009, 2010).

When compared to the base case results from Section 3.1, the OA concentrations for the temperature-sensitive aging case decrease over the northeast and increase over the west. This is consistent with the 298 ± 6 K temperature distribution for this episode wherein western areas are warmer than the northeast, resulting in a slight acceleration and deceleration in aging respectively. On average, total OA concentrations only decrease by about 0.3%. When a temperature increase is applied to the base case, similar results are observed. The OA concentration difference between the temperature-sensitive and temperature-insensitive +5 K cases is shown in Fig. 5. Note that while the scale is relatively small, there are distinct differences. Concentrations are not significantly affected in the northeast, but western and midwestern areas show increased OA levels. These changes are mostly due to aSOA, with some aerosol increase contributed by bSOA and the POA species.

The percent difference between the temperature-sensitive +5 K and base cases for target cities and area averages is shown in Table 3. On average, OA concentrations in the temperature-dependent case decrease by 0.8% in relation to the corresponding base case. In comparison to the difference between the temperature-independent +5 K case and its corresponding base case, the addition of temperature dependence constitutes only a 0.6% increase in total OA (0.1% K^{-1}). This modestly positive departure is also observed in the specified cities, where the difference between temperature-dependent and temperature-independent changes is between 0.3 and 0.7%. Given that a high activation energy was used for these simulations, this is a fairly small change. Therefore, the aging-related OA concentration is only weakly sensitive to temperature in this ground-level scenario.

3.4. Effect of changes in biogenic emissions

As temperature rises, biogenic emissions are also expected to grow. The previous scenarios do not account for this change. Three scenarios were subsequently analyzed: one with a 25% increase in biogenic precursors and a 2.5 K temperature increase (BIO25 + 2.5), another with a 50% increase in emissions for a 5 K increase (BIO50 + 5) and finally a scenario with a 25% increase for +5 K (BIO25 + 5). The maximum temperature during this simulated episode was 32 °C. Adding five degrees, at the upper limit of the IPCC prediction range, brings the maximum temperature up to 37 °C; this is still below 40 °C, the isoprene emissions drop-off temperature (Guenther et al., 1993), indicating that biogenic emissions should only increase and not decrease at any point.

The base case OA was subtracted from the OA in the three biogenic increase cases and the concentration difference maps are shown in Fig. 6b–d. The difference from the base case and the constant biogenic emissions and +5 K case is also shown for comparison (Fig. 6a). While a decrease in southern OA was previously predicted when only temperature was increased, an increase is seen when biogenic precursor emissions increase with temperature. Furthermore, this increase is over an order of magnitude larger than the increase previously seen in the north as a result of chemical aging of aSOA and oPOA.

Table 2 shows concentration change averages and results at specified cities. Unlike previous scenarios, decreases in aerosol are not predicted. On average, total OA concentrations increase by 20.5% for the +5 K and +50% biogenic emissions case,

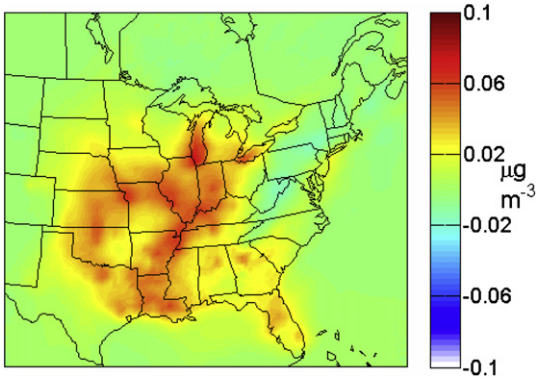

Fig. 5. Total OA concentration difference between the AGE + 5 and TEMP + 5 cases to assess the importance of having a temperature-dependent aging rate constant.

Table 3
Predicted total OA changes in select cities for the AGE scenarios.

Site	Base case concentration, μg m^{-3}	Percent difference between AGE + 5 and AGE_Base[a]	% Difference from TEMP + 5 case[b]
Average	3.1	−0.8%	0.6%
Hattiesburg, MS	9.1	−3.8%	0.4%
Atlanta, GA	11.8	−2.6%	0.6%
Shreveport, LA	11.1	−2.9%	0.4%
Cincinnati, OH	8.1	2.2%	0.7%
Pittsburgh, PA	6.0	0.6%	0.3%
Chicago, IL	10.5	0.7%	0.7%

[a] [(AGE + 5 − AGE_Base)/AGE_Base].
[b] Difference between the AGE percent changes (AGE + 5 − AGE_Base) and those found for the TEMP + 5 − Base case in Table 2. [(AGE + 5 − AGE_Base) − (TEMP + 5 − Base)]/(Base).

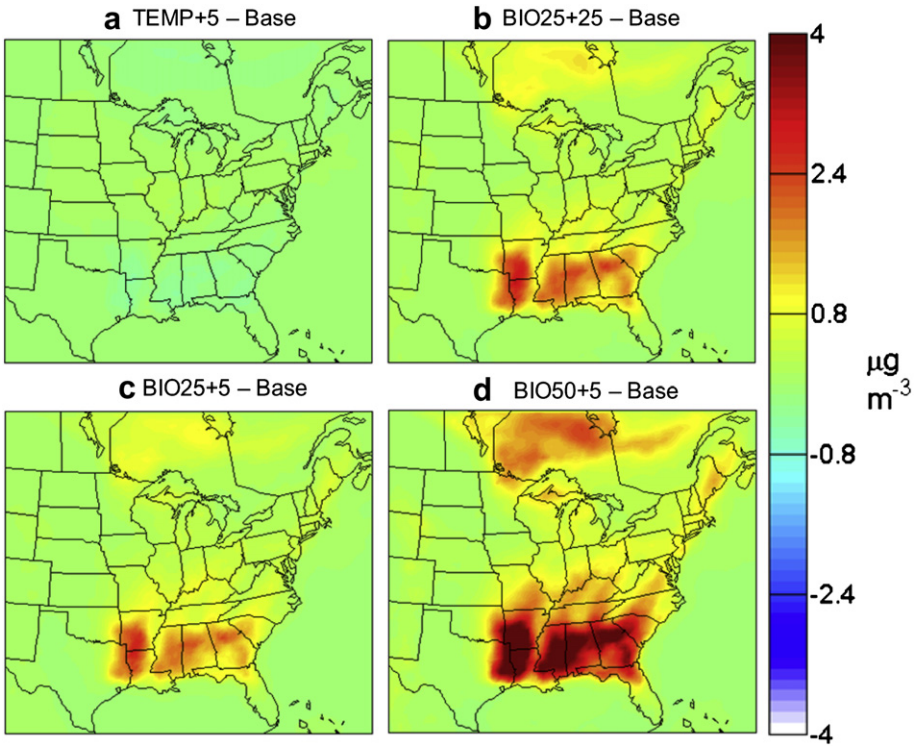

Fig. 6. Total OA concentration maps showing the deviation from base of (a) TEMP + 5, the +5 K case, (b) BIO25 + 25, the +2.5 K and +25% biogenic emissions case, (c) BIO25 + 5, the +5 K and +25% biogenic emissions case, and (d) BIO50 + 5, the +5 K and +50% biogenic emissions case.

compared to −1.5% for the +5 K-only case. The greatest effect is in Shreveport, LA for the +5 K and +50% biogenic emissions case, wherein the total OA increases by 47% over the base case. Each scenario with biogenic increases shows a much larger increase in aerosol compared to the <5% changes that have been previously discussed.

Both +25% biogenic emissions simulations have similar difference values even though the temperature differences are not the same (Table 2, Fig. 6b and c). The increased biogenic emissions therefore appear to dominate the impact on OA concentration. In reality, the behavior of biogenic emissions with temperature is more complex than a simplistic percentage per Kelvin change, and so including more accurate biogenic emissions temperature sensitivity (Guenther et al., 2006) is important for more accurate estimates.

In order to check the accuracy of the BIO scenario results, predicted changes at specific sites were divided by respective temperature changes for comparison to the observations of Leaitch et al. (in press) (Fig. 7). The change in submicron forest OA at 23 and 28 °C — which were the simulation averages during the base and +5 K cases — is calculated to be 0.25 and 0.50 μg m^{-3} K^{-1} respectively based upon the Leaitch et al. (in press) equation described previously. These values are shown as red dotted lines in Fig. 7. The Canadian forests are different than biogenically-dominated sites in the southern U.S., but comparison with these results serves to show whether the PMCAMx-2008 predictions are reasonable. In the first three cities, which are biogenically dominated, the +5 K and +25% biogenic emissions case is close to observations. The last three cities exhibit much lower OA changes than Leaitch et al. (in press) estimates; as discussed, the OA in northern areas is predicted to have a large anthropogenic component and is therefore less sensitive to changes in biogenic emissions.

The volatility distribution differences between the base and +5 K and +25% biogenic emissions case for bSOA and aSOA are shown in Fig. 8. Noting the increased *y*-axes compared to Fig. 4, total bSOA increases in all bins, which is not surprising given that its precursor concentration has been enhanced by 25%. Doing so increases the available biogenic semi-volatile gases and, due to equilibrium partitioning, causes material to partition into the aerosol phase. The change in aSOA, however, follows a different

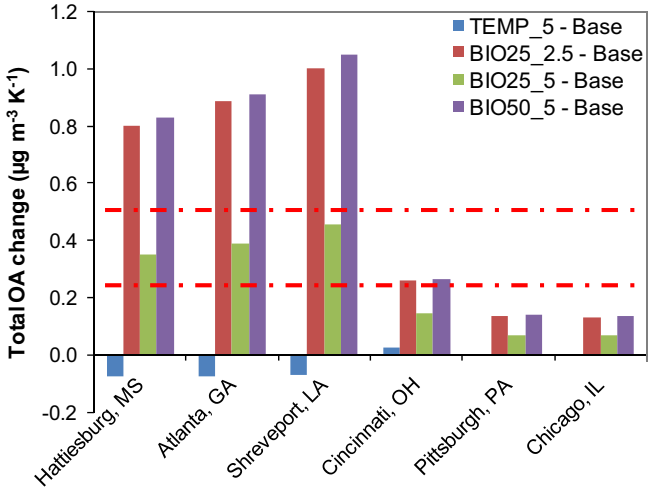

Fig. 7. OA concentration change between BIO and Base scenarios per degree for specific cities. Red lines indicate 0.25 and 0.50 μg m^{-3} K^{-1}, which correspond to OM at 23 and 28 °C as determined by Leaitch et al. (in press). (For interpretation of the references to color in this figure legend, the reader is referred to the web version of this article.)

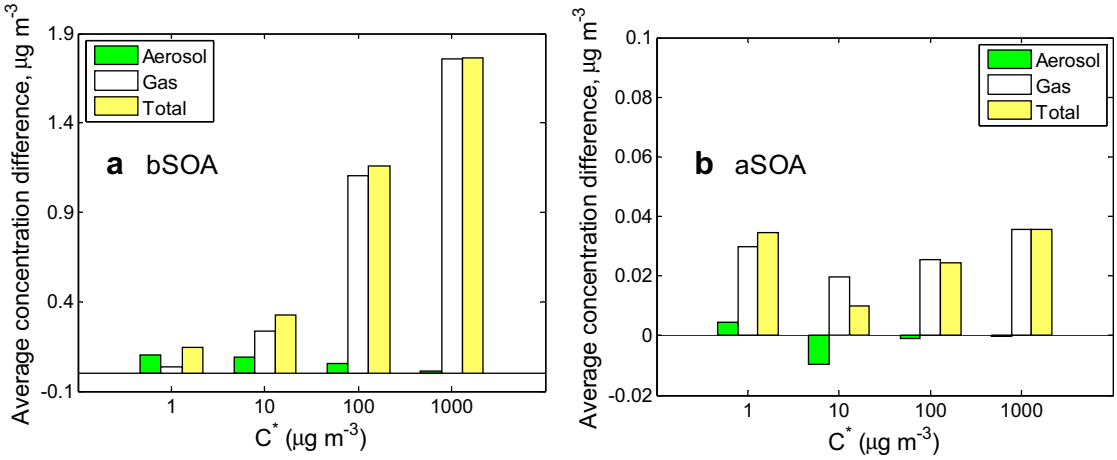

Fig. 8. Volatility plots showing the difference between BIO25 + 5 and base cases for (a) bSOA and (b) aSOA. Note that *y*-axes are not the same for both species.

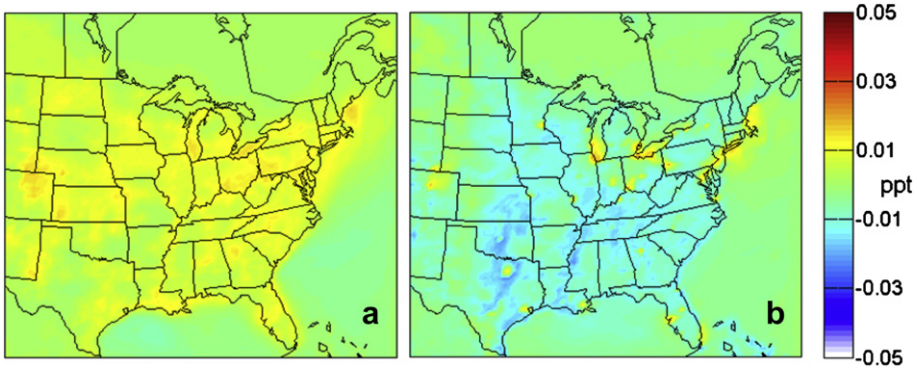

Fig. 9. Concentration maps of OH differences between (a) TEMP + 5 and Base and (b) BIO50 + 5 and Base.

pattern. More gas is staying in the upper volatility bins and less aerosol is being formed in the lower bins. This indicates that aging has slowed down after the increase of biogenic emissions. The POA behavior is similar to the previous case, but the aSOA behavior instigates investigation into the OH levels, as these control aging in this scenario.

The effect of increasing temperature and biogenic emissions on the OH concentrations is shown in Fig. 9. Increasing temperature results in a general increase in OH; +7% on average, ranging between −5% and +18%. Different behavior is observed in Fig. 9b; the OH concentration still increases in the major urban areas, but there are prevalent areas of OH decrease across the eastern U.S. when the biogenic emission rates are increased with temperature. The average change is −9%, ranging between −25% and +25%. Additional biogenic VOCs therefore decrease the availability of OH, thereby reducing the aSOA ability to age and accumulate more aerosol.

3.5. Linearity of changes

The +2.5 K simulation yielded results with the same spatial pattern of changes as the +5 K simulation, with a 0.2% average increase in the north and a 1.3% decrease in the south (versus 0.7% and −2.6% respectively for the +5 K case). These changes are linear in the south and close to linear in the north (Table 4). The changes are also close to linear in the cases where the biogenic emissions are allowed to increase (Table 4).

3.6. Change of OA Aloft

The north-south disparity observed in Section 3.2 is also seen with increasing altitude (Fig. 10a–c). Aerosol concentrations at southern, biogenic-dominated areas decrease at the surface but the effect decays rapidly with height, while the increase in aerosol concentration at anthropogenic-dominated sites in the north persist to higher altitudes as more precursors oxidize and condense out of the gas phase. Additional oxidized aerosol may lead to increased formation of cloud droplets (Jimenez et al., 2009), and so chemical aging may have consequences not only on health at the surface but on radiative forcing at higher altitudes as well. When biogenic emissions are increased with temperature, however, bSOA dominates the increase not only in southern cities but in northern sites as well (Fig. 10d and e). The biogenic effect again decreases quickly with altitude, only affecting the lower

Table 4
Predicted differences of OA concentration change (as a percentage) between scenarios.

Scenarios compared	Concentration change		
	Average	North	South
TEMP + 25 − Base (+2.5 K)	−0.8%	0.2%	−1.3%
TEMP + 5 − Base (+5 K)	−1.5%	0.7%	−2.6%
BIO25 + 25 − Base (+2.5 K)	9.9%	6.2%	17.3%
BIO50 + 5 − Base (+5 K)	20.5%	13.0%	36.1%

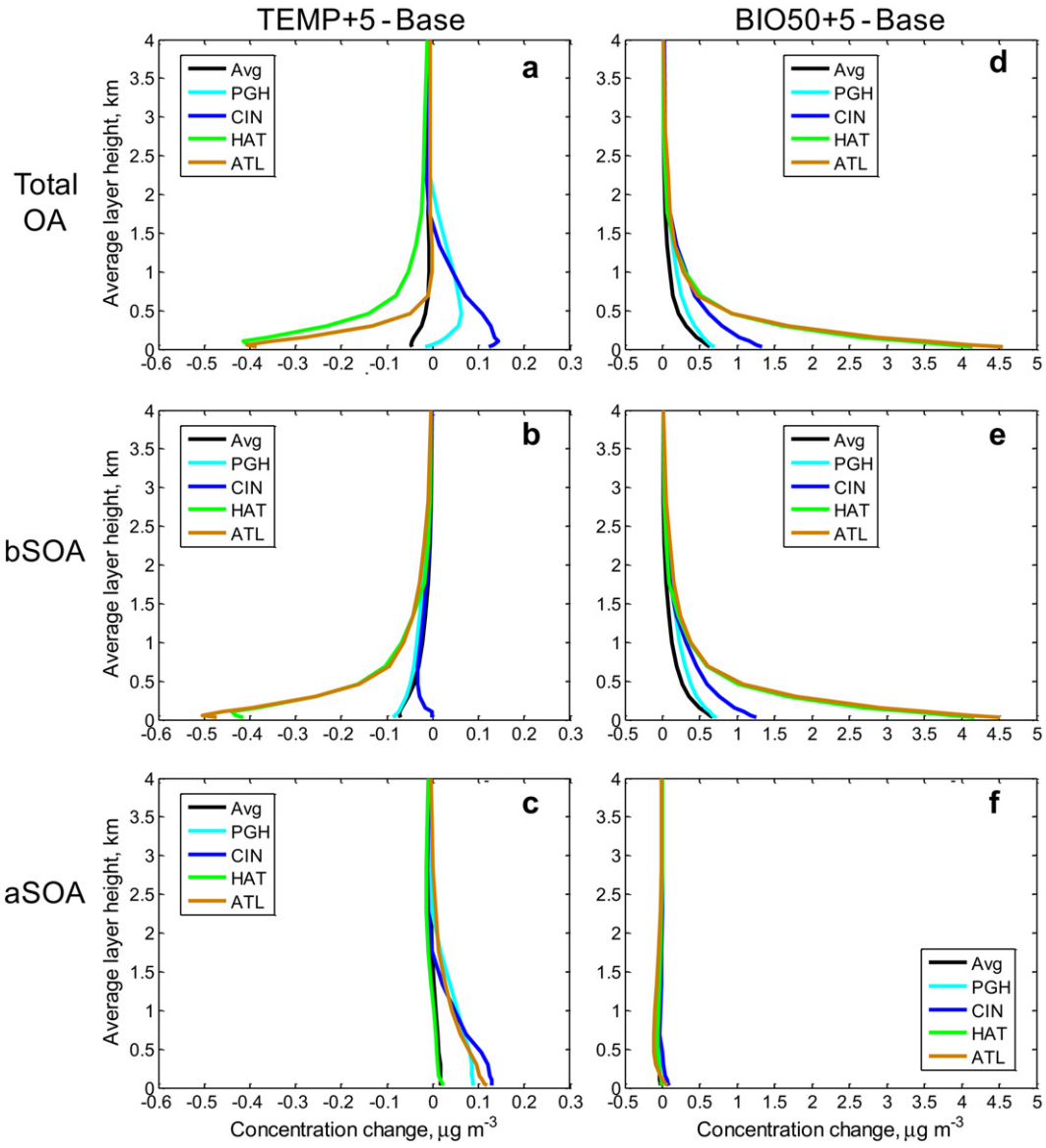

Fig. 10. Vertical concentration profile of total OA (a,d), bSOA (b,e), and aSOA (c,f) changes between the TEMP + 5 − base (a–c) and BIO50 + 5 − Base (d–f) cases. Hattiesburg (HAT) and Atlanta (ATL) are biogenically-dominated cities; Cinncinati (CIN) and Pittsburgh (PGH) are anthropogenically-dominated cities.

kilometer. Anthropogenic aging decelerates due to the decrease in OH and does not contribute significant to aerosol change over any cities (Fig. 10f).

4. Conclusions

Increasing temperature has a variety of effects on organic aerosol concentrations. If temperature alone is increased, bSOA and fPOA will generally evaporate and decrease in concentration. This leads to an average decrease in the South US of 0.4% K^{-1}. While an increase in temperature also causes the evaporation of aSOA and oPOA, the corresponding species continue to react with OH due to chemical aging. This decreases the volatility of the resultant OA components; as a result, an effective increase in the aging aerosols is predicted, leading to an increase in the north of about 0.3% K^{-1}. Making the aging rate constant temperature-sensitive with a high Arrhenius E_a/R value of 500 K resulted in a 0.1% K^{-1} difference from the TEMP + 5 case. The temperature dependence of aerosol aging does not appear to have a significant impact.

The temperature dependence of biogenic precursor emissions, however, has a critical effect on PMCAMx-2008 OA change predictions. Total aerosol concentrations increased for all augmented biogenic emission cases, up to almost 10% K^{-1} in some southern cities. The concentration change with temperature for these same cities was fairly consistent with field observations by Leaitch et al. (in press). Increased biogenic emissions also resulted in lower OH concentrations, leading to decreased aging of aSOA and oPOA. These changes due to aging were of a much smaller magnitude than the bSOA concentration increase, however. Repeating these trials with a more realistic biogenic emissions model is recommended for future work.

Other research shows that biogenic emissions may be limited via plant response to elevated levels of CO_2 and changing land use/land cover (Arneth et al., 2008; Heald et al., 2009; Guenther et al., 2006; Chen et al., 2009). Our study only takes into account the temperature effect of climate change, and other factors should be addressed. The potential sensitivity of biogenic systems to climate

change in this work, however, suggests that their response will dominate the effects of climate change on air quality.

Acknowledgments

This research was supported by the EPA STAR program through the National Center for Environmental Research (NCER). This paper has not been subject to the EPA's peer and policy review, and therefore does not necessarily reflect the views of the Agency. No official endorsement should be inferred. Melissa Day was supported by a National Science Foundation Graduate Research Fellowship and an Achievement Rewards for College Scientists (ARCS) Scholarship.

References

Arneth, A., Schurgers, G., Hickler, T., Miller, P.A., 2008. Effects of species composition, land surface cover, CO_2 concentration and climate on isoprene emissions from European forests. Plant Biology 10, 150–162.

Aw, J., Kleeman, M.J., 2003. Evaluating the first-order effect of intraannual temperature variability on urban air pollution. Journal of Geophysical Research 108, 4365. doi:10.1029/2002JD002688.

Baertsch-Ritter, N., Keller, J., Dommen, J., Prevot, A.S.H., 2004. Effects of various meteorological conditions and spatial emission resolutions on the ozone concentration and ROG/NO_x limitation in the Milan area (I). Atmospheric Chemistry and Physics 4, 423–438.

Carter, W.P.L., 2000. Documentation of the SAPRC-99 Chemical Mechanism for VOC Reactivity Assessment. Final Report to California Air Resources Board Contract No. 92–329, and 95–308. http://www.cert.ucr.edu/%7ecarter/absts.htm#saprc99.

Chen, J., Avise, J., Guenther, A., Wiedinmyer, C., Salathe, E., Jackson, R.B., Lamb, B., 2009. Future land use and land cover influences on regional biogenic emissions and air quality in the United States. Atmospheric Environment 43, 5771–5780.

Chow, J.C., Watson, J.G., Crow, D., Lowenthal, D.H., Merrifield, T., 2001. Comparison of IMPROVE and NIOSH carbon measurements. Aerosol Science and Technology 34, 23–34.

Constable, J.V.H., Guenther, A.B., Schimel, D.S., Monson, R.K., 1999. Modeling changes in VOC emissions in response to climate change in the continental United States. Global Change Biology 5, 791–806.

Davidson, C.I., Phalen, R.F., Solomon, P.A., 2005. Airborne particulate matter and human health: a review. Aerosol Science and Technology 39 (8), 737–749.

Dawson, J.P., Adams, P.J., Pandis, S.N., 2007. Sensitivity of $PM_{2.5}$ to climate in the Eastern US: a modeling case study. Atmospheric Chemistry and Physics 7, 4295–4309.

Dawson, J.P., Racherla, P.N., Lynn, B.H., Adams, P.J., Pandis, S.N., 2008. Simulating present-day and future air quality as climate changes: model evaluation. Atmospheric Environment 42, 4551–4566.

Dawson, J.P., Racherla, P.N., Lynn, B.H., Adams, P.J., Pandis, S.N., 2009. Impacts of climate change on regional and urban air quality in the eastern United States: role of meteorology. Journal of Geophysical Research 114, D05308. doi:10.1029/2008JD009849.

Dockery, D.W., Pope III, C.A., 1994. Acute respiratory effects of particulate air pollution. Annual Review of Public Health 15, 107–132.

Donahue, N.M., Robinson, A.L., Stanier, C.O., Pandis, S.N., 2006. Coupled partitioning, dilution, and chemical aging of semivolatile organics. Environmental Science & Technology 40, 2635–2643.

Duncan, B.N., Yoshida, Y., Damon, M.R., Douglass, A.R., Wittel, J.C., 2009. Temperature dependence of factors controlling isoprene emissions. Geophysical Research Letters 36, L05813. doi:10.1029/2008GL037090.

Epstein, S., Riipinen, I., Donahue, N., 2010. A semiempirical correlation between enthalpy of vaporization and saturation concentration for organic Aerosol. Environmental Science & Technology 44, 743–748.

Gaydos, T.M., Pinder, R., Koo, B., Fahey, K.M., Yarwood, G., Pandis, S.N., 2007. Development and application of a three-dimensional aerosol chemical transport model, PMCAMx. Atmospheric Environment 41, 2594–2611.

Gery, M.W., Whitten, G.Z., Killus, J.P., Dodge, M.C., 1989. A photochemical kinetics mechanism for urban and regional scale computer modeling. Journal of Geophysical Research 94, 925–956. doi:10.1029/JD094iD10p12925.

Grell, G.A., Dudhia, J., Stauffer, D.R., 1995. A Description of the Fifth-generation Penn State/NCAR Mesoscale Model (MM5). NCAR/TN-398 + STR. National Center for Atmospheric Research, Boulder, CO. http://www.mmm.ucar.edu/mm5/documents/mm5-desc-doc.html.

Grieshop, A.P., Logue, J.M., Donahue, N.M., Robinson, A.L., 2009. Laboratory investigation of photochemical oxidation of organic aerosol from wood fires: 1. Measurement and simulation of organic aerosol evolution. Atmospheric Chemistry and Physics 9, 1263–1277.

Guenther, A.B., Zimmerman, P.R., Harley, P.C., Monson, R.K., Fall, R., 1993. Isoprene and monoterpene emission rate variability: model evaluations and sensitivity analyses. Journal of Geophysical Research 98 (D7), 12,609–12,617. doi:10.1029/93JD00527.

Guenther, A., Karl, T., Harley, P., Wiedinmyer, C., Palmer, P.I., Geron, C., 2006. Estimates of global terrestrial isoprene emissions using MEGAN (Model of Emissions of Gases and Aerosols from Nature). Atmospheric Chemistry and Physics 6, 3181–3210.

Heald, C.L., Wilkinson, M.J., Monson, R.K., Alo, C.A., Wang, G., Guenther, A., 2009. Response of isoprene emission to ambient CO_2 changes and implications for global budgets. Global Change Biology 15, 1127–1140.

Hildebrandt, L., Donahue, N.M., Pandis, S.N., 2009. High formation of secondary organic aerosol from the photo-oxidation of toluene. Atmospheric Chemistry and Physics 9, 2973–2986.

IMPROVE, 1995. IMPROVE Data Guide, August, 1995. University of California Davis, Davis, CA. http://vista.cira.colostate.edu/improve/Publications/OtherDocs/IMPROVEDataGuide/IMPROVEDataGuide.htm.

Intergovernmental Panel on Climate Change (IPCC), 2007. Climate Change 2007: The Physical Science Basis. Cambridge University Press, Cambridge, UK and New York, NY, USA.

Jacob, D., Winner, D., 2009. Effect of climate change on air quality. Atmospheric Environment 43, 51–63.

Jimenez, J.L., Canagaratna, M.R., Donahue, N.M., Prevot, A.S.H., Zhang, Q., Kroll, J.H., DeCarlo, P.F., Allan, J.D., Coe, H., Ng, N.L., Aiken, A.C., Docherty, K.S., Ulbrich, I.M., Grieshop, A.P., Robinson, A.L., Duplissy, J., Smith, J.D., Wilson, K.R., Lanz, V.A., Hueglin, C., Sun, Y.L., Tian, J., Laaksonen, A., Raatikainen, T., Rautiainen, J., Vaattovaara, P., Ehn, M., Kulmala, M., Tomlinson, J.M., Collins, D.R., Cubison, M.J., Dunlea, E.J., Huffman, J.A., Onasch, T.B., Alfarra, M.R., Williams, P.I., Bower, K., Kondo, Y., Schneider, J., Drewnick, F., Borrmann, S., Weimer, S., Demerjian, K., Salcedo, D., Cottrell, L., Griffin, R., Takami, A., Miyoshi, T., Hatakeyama, S., Shimono, A., Sun, J.Y., Zhang, Y.M., Dzepina, K., Kimmel, J.R., Sueper, D., Jayne, J.T., Herndon, S.C., Trimborn, A.M., Williams, L.R., Wood, E.C., Middlebrook, A.M., Kolb, C.E., Baltensperger, U., Worsnop, D.R., 2009. Evolution of organic aerosols in the atmosphere. Science 326, 1525–1529.

Kanakidou, M., Seinfeld, J.H., Pandis, S.N., Barnes, I., Dentener, F.J., Facchini, M.C., van Dingenen, R., Ervens, B., Nenes, A., Nielsen, C.J., Swietlicki, E., Putaud, J.P., Balkanski, Y., Fuzzi, S., Horth, J., Moortgat, G.K., Winterhalter, R., Myhre, C.E.L., Tsigaridis, K., Vignati, E., Stephanou, E.G., Wilson, J., 2005. Organic aerosol and global climate modelling: a review. Atmospheric Chemistry and Physics 5, 1053–1123.

Karydis, V.A., Tsimpidi, A.P., Pandis, S.N., 2007. Evaluation of a three-dimensional chemical transport model (PMCAMx) in the eastern United States for all four seasons. Journal of Geophysical Research 112, D14211. doi:10.1029/2006JD007890.

Lamb, B., Guenther, A., Gay, D., Westberg, H., 1987. A national inventory of biogenic hydrocarbon emissions. Atmospheric Environment 21 (8), 1695–1705.

Lane, T.E., Donahue, N.M., Pandis, S.N., 2008. Simulating secondary organic aerosol formation using the volatility basis-set approach in a chemical transport model. Atmospheric Environment 42, 7439–7451.

Leaitch W.R., Macdonald A.M., Brickell P.C., Liggio J., Sjostedt S.J., Vlasenko A., Bottenheim J.W., Huang L., Li S.-M., Liu P.S.K., Toom-Sauntry D., Hayden K.A., Sharma S., Shantz N.C., Wiebe H.A., Zhang W., Abbatt, J.P.D., Slowik J.G., Chang R.Y.-W., Russell L.M., Schwartz R.E., Takahama S., Jayne J.T., Ng N.L. Temperature response of the submicron organic aerosol from temperate forests. Atmospheric Environment, in press, doi:10.1016/j.atmosenv.2011.08.047.

Murphy, B., Pandis, S.N., 2009. Simulating the formation of semivolatile primary and secondary organic aerosol in a regional chemical transport model. Environmental Science and Technology 43, 4722–4728.

Murphy, B., Pandis, S.N., 2010. Exploring summertime organic aerosol formation in the eastern United States using a regional-scale budget approach and ambient measurements. Journal of Geophysical Research 115, D24216. doi:10.1029/2010JD014418.

Nenes, A., Pandis, S.N., Christodoulos, P., 1998. ISORROPIA: a new thermodynamic equilibrium model for multiphase multicomponent inorganic aerosols. Aquatic Geochemistry 4, 123–152.

Odum, J., Hoffman, T., Bowman, F., Collins, D., Flagan, R.C., Seinfeld, J.H., 1996. Gas/particle partitioning and secondary organic aerosol yields. Environmental Science & Technology 30, 2580–2585.

Robinson, A.L., Donahue, N.M., Shrivastava, M.K., Weitkamp, E.A., Sage, A.M., Grieshop, A.P., Lane, T.E., Pierce, J.R., Pandis, S.N., 2007. Rethinking organic aerosol: semivolatile emissions and photochemical aging. Science 315, 1259–1262.

Schwede, D., Pouliot, G., Pierce, T., 2005. Changes to the Biogenic Emissions Inventory System Version 3 (BEIS3) 2005, Paper Presented at 4th Annual CMAS User's Conference, Friday Center. UNC-Chapel Hill, NC. 26–28 Sept. http://www.cmascenter.org/conference/2005/abstracts/2_7.pdf.

Seinfeld, J.H., Pandis, S.N., 2006. Atmospheric Chemistry and Physics: From Air Pollution to Climate Change, second ed.. John Wiley and Sons, Hoboken, NJ.

Sharkey, T.D., Wiberley, A.E., Donohue, A.R., 2008. Isoprene emission from plants: why and how. Annals of Botany 101, 5–18.

Sheehan, P.E., Bowman, F.M., 2001. Estimated effects of temperature on secondary organic aerosol concentrations. Environmental Science and Technology 35, 2129–2135.

Shrivastava, M.K., Lane, T.E., Donahue, N.M., Pandis, S.N., Robinson, A.L., 2008. Effects of gas-particle partitioning and aging of primary emissions on urban and regional organic aerosol concentrations. Journal of Geophysical Research 113, D18301. doi:10.1029/2007JD009735.

Simon, H., Bhave, P.V., Swall, J.L., Frank, N.H., Malm, W.C., 2011. Determining the spatial and seasonal variability in OM/OC ratios across the US using multiple regression. Atmospheric Chemistry and Physics 11, 2933–2949.

Strader, R., Lurmann, F., Pandis, S.N., 1999. Evaluation of secondary organic aerosol formation in winter. Atmospheric Environment 33, 4849–4863.

Tai, A.P.K., Mickley, L.J., Jacob, D.J., 2010. Correlations between fine particulate matter ($PM_{2.5}$) and meteorological variables in the United States: implications for the sensitivity of $PM_{2.5}$ to climate change. Atmospheric Environment 44 (32), 3976–3984.

U.S. EPA, April 2002. User Guide: Air Quality System. http://www.epa.gov/ttn/airs/aqs/softw/AQSUserGuide_v1.pdf.

Zhang, Q., Worsnop, D.R., Canagaratna, M.R., Jimenez, J.L., 2005. Hydrocarbon-like and oxygenated organic aerosols in Pittsburgh: insights into sources and processes of organic aerosols. Atmospheric Chemistry and Physics 5, 3289–3311.